HHS Public Access

Author manuscript

Am J Sports Med. Author manuscript; available in PMC 2023 July 01.

Published in final edited form as:

Am J Sports Med. 2022 July ; 50(8): 2281–2291. doi:10.1177/03635465221097939.

Mesenchymal Stem Cell Delivery via Topographically Tenoinductive Collagen Biotextile Enhances Regeneration of Segmental Tendon Defects

Phillip McClellan, PhD[*], **Jason G. Ina, MD**[†], **Derrick M. Knapik, MD**[†], **Ilaha Isali, MD**[‡], **Greg Learn, BS**[§], **Alexis Valente, BS**[*], **Yujing Wen**[*], **Ruiqi Wen**[§], **James M. Anderson, MD, PhD**[§,||,¶], **Robert J. Gillespie, MD**[†], **Ozan Akkus, PhD**[*,†,§,#]

[*]Department of Mechanical and Aerospace Engineering, Case Western Reserve University, Cleveland, Ohio, USA.

[†]Department of Orthopaedic Surgery, University Hospitals Cleveland Medical Center, Ohio, USA.

[‡]Department of Urology, Case Western Reserve University, Cleveland, Ohio, USA.

[§]Department of Biomedical Engineering, Case Western Reserve University, Cleveland, Ohio, USA.

[||]School of Medicine, Case Western Reserve University, Cleveland, Ohio, USA.

[¶]Department of Pathology, Case Western Reserve University, Cleveland, Ohio, USA.

Abstract

Background: Successful management of massive rotator cuff (RC) tendon tears represents a treatment challenge because of the limited intrinsic healing capacity of native tendons and the risk of repair failure. Biologic augmentation of massive RC tears utilizing scaffolds—capable of regenerating bulk tendon tissue to achieve a mechanically functional repair—represents an area of increasing clinical interest.

Purpose: To investigate the histological and biomechanical outcomes after the use of a novel biologic scaffold fabricated from woven electrochemically aligned collagen (ELAC) threads as a suture-holding, fully load-bearing, defect-bridging scaffold with or without mesenchymal stem cells (MSCs) compared with direct repair in the treatment of critically sized RC defects using a rabbit model.

Study Design: Controlled laboratory study.

[#]Address correspondence to Ozan Akkus, PhD, Kent H. Smith, Prof., Department of Mechanical and Aerospace Engineering, Department of Biomedical Engineering, Department of Orthopaedic Surgery, Case Western Reserve University, 2123 Martin Luther King Junior Boulevard, Cleveland, OH 44106, USA (oxa@case.edu).

One or more of the authors has declared the following potential conflict of interest or source of funding: J.G.I. has received support for education from Rock Medical Orthopedics. D.M.K. has received a grant from Arthrex and support for education from Smith & Nephew and Medwest Associates. J.M.A. has received consulting fees from Medtronic Vascular and Bayer HealthCare Pharmaceuticals. R.J.G. has received consulting fees from Stryker, DJO Global, Shoulder Innovations, Encore Medical, and Aevumed and royalties from Shoulder Innovations; he has ownership in Collamedix Inc. AOSSM checks author disclosures against the Open Payments Database (OPD). AOSSM has not conducted an independent investigation on the OPD and disclaims any liability or responsibility relating thereto.

Methods: A total of 34 New Zealand White rabbits underwent iatrogenic creation of a critically sized defect (6 mm) in the infraspinatus tendon of 1 shoulder, with the contralateral shoulder utilized as an intact control. Specimens were divided into 4 groups: (1) gap—negative control without repair; (2) direct repair of the infraspinatus tendon—operative control; (3) tendon repair using ELAC; and (4) tendon repair using ELAC + MSCs. Repair outcomes were assessed at 6 months using micro–computed tomography, biomechanical testing, histology, and immunohistochemistry.

Results: Specimens treated with ELAC demonstrated significantly less tendon retraction when compared with the direct repair group specimens ($P = .014$). ELAC + MSCs possessed comparable biomechanical strength (178 ± 50 N) to intact control shoulders (199 ± 35 N) ($P = .554$). Histological analyses demonstrated abundant, well-aligned de novo collagen around ELAC threads in both the ELAC and the ELAC + MSC shoulders, with ELAC + MSC specimens demonstrating increased ELAC resorption (7% vs 37%, respectively; $P = .002$). The presence of extracellular matrix components, collagen type I, and tenomodulin, indicating tendon-like tissue formation, was appreciated in both the ELAC and the ELAC + MSC groups.

Conclusion: The application of MSCs to ELAC scaffolds improved biomechanical and histological outcomes when compared with direct repair for the treatment of critically sized defects of the RC in a rabbit model.

Clinical Relevance: This study demonstrates the feasibility of repairing segmental tendon defects with a load-bearing, collagen biotextile in an animal model, showing the potential applicability of RC repair supplementation using allogeneic stem cells.

Keywords

biologic healing enhancement; rotator cuff; stem cell therapy; tissue engineering

Rotator cuff (RC) tendon injuries represent the most common pathology of the shoulder managed by orthopaedic surgeons,[36] with up to 70% of shoulder-related visicts reported to involve the RC.[35,37] RC injuries represent a substantial cause of pain and disability in patients of all ages,[15] with approximately 330,000 RC procedures performed annually in the United States alone.[8] Because of the limited intrinsic healing capacity of RC tendons after injury, surgical repair is often required after a trial of nonoperative management to restore shoulder function and strength, while eliminating pain.[9] In patients with large to massive RC tears—defined by tears with ≥5 cm tendon retraction or involvement of ≥2 tendons—the risk for repair failure and recurrent tearing is high because of inferior tissue quality or excess stress placed across the repair site.[12] Moreover, in the setting of chronic RC tears, successful repair becomes increasingly challenging because of the loss of bulk tendon tissue via muscular atrophy, tissue fibrosis, and fatty infiltration,[5,14,25,43] limiting the effectiveness of current repair strategies.[39] Tissue engineering scaffolds have been investigated to help restore the anatomic footprint of the RC tendons on the proximal humerus, improving mechanical strength while providing a framework to promote biological healing when a primary repair is not feasible.[13]

As the native extracellular matrix of the RC tendons is composed of collagen, collagen-based biomaterials have been suggested to be the most suitable materials for native

tendon replacement and regeneration.[3,11,21,44] While previous scaffold systems composed predominately of collagen may function as vehicles for cell delivery, extensive culture times in vitro have been reported as necessary to achieve an acceptable degree of mechanical robustness to effectively bridge segmental defects between muscle and bone.[4,16,26] Recently, our group introduced a novel, collagen-based biomaterial capable of generating collagen fibers via the biofabrication process of electrochemical compaction.[7,24,42] These electrochemically aligned collagen (ELAC) threads can then be woven together to construct biotextile scaffolds.[27] ELAC scaffolds have been shown to exhibit biomechanical properties comparable with native RC tendon,[1,19] while possessing the intrinsic ability to induce tenogenic differentiation of mesenchymal stem cells (MSCs) in vitro in the absence of exogenous growth factors[23,45] by promoting cytoskeletal and nuclear elongation.[20] Results of a recent pilot study examining the use of woven ELAC scaffolds seeded with and without MSCs in full load-bearing capacity to bridge surgically induced, acute massive RC defects in a rabbit model found that at 3 months, MSC-seeded ELAC scaffolds demonstrated superior repair stiffness relative to nonseeded scaffold repairs.[27] Moreover, histological staining demonstrated robust collagen deposition after ELAC implantation in scaffolds with and without MSCs.[27]

While the applicability of MSC delivery on ELAC scaffolds for tendon regeneration has been demonstrated,[27] the previous investigation was exploratory and limited by the use of a small number of specimens with a shortterm follow-up. The purpose of the present study was to assess the long-term regenerative potential of MSC delivery via woven ELAC scaffolds for the treatment of critically sized RC tears in a rabbit model based on repair healing biomechanics, scaffold remodeling, and typification of regenerated extracellular matrix. We hypothesized that ELAC scaffolds would be superior to the operative standard (direct repair) in terms of histological and biomechanical properties and that supplementation of ELAC scaffolds with MSCs would yield further histological and biomechanical improvements.

METHODS

Study Design

The objective of this study was to investigate an RC repair strategy to evaluate the long-term regeneration of bulk tendon tissue utilizing scaffolds composed of ELAC, as well as to assess the capacity of ELAC scaffolds as an MSC delivery vehicle. A total of 34 New Zealand White rabbits were utilized for the study, with each specimen undergoing iatrogenic creation of a critically sized defect (6 mm) to the infraspinatus tendon except for those in the direct repair group. Specimens were divided into 1 of 4 groups (Figure 1): (1) gap—negative control, (2) direct repair—operative control, (3) ELAC, and (4) ELAC + MSCs. Scaffolds were implanted to span the critically sized defect created in the infraspinatus tendon. MSCs utilized were allogenic and isolated from 3 skeletally mature adult female New Zealand White rabbits not included in the analysis to minimize biological variation. Histological and biomechanical outcomes were analyzed after euthanasia 6 months after surgery.

Scaffold Fabrication, MSC Isolation and Seeding, and Operative Procedures

Scaffolds were fabricated as described previously,[27] and details regarding the fabrication process are provided in the Appendix (available in the online version of this article). Similarly, MSC isolation and surgical procedures were conducted under the appropriate Institutional Animal Care and Use Committee approvals at Case Western Reserve University in a fashion similar to previous work,[27] and detailed protocols and images are included in Appendix Figures A1 and A2 (available online).

Micro–Computed Tomography

After euthanasia, the scapulohumeral complex from each specimen was harvested bilaterally and imaged using micro–computed tomography (microCT) (Siemens Inveon PET/CT; Siemens Medical Solutions. 75–80 kV, 470–500 ma, 630- to 670-millisecond exposure, 42-μm voxel edge lengths) in the scapular plane. Tendon or scaffold retraction measurements were assessed in specimens based on the migration of the stainless steel suture marker. The initial appearance of the scapular spine bifurcation was set as the origin (0 mm) for measurements, and the initial appearance of the stainless steel suture (progressing from the proximal to the distal slice) was marked as the suture location. Additionally, 3-dimensional reconstructions of the scapula, humeral head, and stainless steel suture from representative specimens in each group were generated from Digital Imaging and Communications in Medicine files in 3D Slicer (slicer.org[22]), with bone (1500–7000) and stainless steel suture (>7500) thresholds set based on visual assessment. Harvested tissues were then stored at −20°C until biomechanical testing or fixed in 10% neutral buffered formalin for histological assessment.

Biomechanical Testing

A predetermined number of specimens from each group were allocated for biomechanical testing (Figure 1). Humeri were potted in aluminum blocks using acrylic cement (Millenium Pour; Keystone Industries), and tissues were kept hydrated using phosphate buffered saline–soaked gauze at all times. Aluminum blocks were clamped in place; the infraspinatus muscle was anchored to dry ice–cooled grips and pulled perpendicular to the insertion of the original enthesis in line with the fibers of the native tendon (Appendix Figure A3, available online) under monotonic tension at 10 mm/min (Test Resources 800LE3–2; Test Resources Inc).

Structural Mechanical Properties—Stiffness and peak load values were extracted from load-displacement data, and failure location was noted (tendon-bone junction vs midsubstance). Values from the operative shoulder (gap, n = 4; direct repair, n = 6; ELAC, n = 7; ELAC + MSCs, n = 7) and the intact contralateral shoulder of each animal were collected to account for rabbit to rabbit variations in tendon strength. A linear regression analysis was performed on the elastic regions of load-displacement curves from 40% to 60% of the peak load value, and the slope of the best-fit line was taken to be stiffness ($R^2 \geq 0.95$).

Tissue-Level Mechanical Properties—Apparent modulus and stress were calculated for a subset of specimens (direct repair, n = 4; ELAC, n = 4; and ELAC + MSCs, n = 5). Not

all samples that underwent biomechanical testing were included because not all specimens were available for tissue thickness and width measurements.

Histology and Immunohistochemistry

The predetermined number of harvested specimens (gap, n = 2; direct repair, n = 2; ELAC, n = 3; ELAC + MSCs, n = 3) were fixed (10% NBF; Fisher Scientific), decalcified (Immunocal; Statlab Medical Products), processed, and embedded in paraffin. Sections (5 μm thickness) were stained, imaged using a microscope (Olympus IX83; Olympus Corp), and assessed for collagen deposition (Masson trichrome [MT]), collagen alignment (picrosirius red [PSR]), cellularity, and cell structure (hematoxylin and eosin). ELAC and ELAC + MSC groups were divided further into 2 categories: “inside,” referring to regions within the continuum of the scaffold, and “outside,” denoting regions within the tissue surrounding the scaffold material. More details regarding sample preparation and section selection can be found in the Appendix.

De novo Collagen Content and Scaffold Resorption—MT-stained slides were assessed using stereological point counting[30,31,40] to determine overall collagen content. A grid (200 × 200 μm) was overlaid onto images collected from slides (Appendix Figure A4, available online), and points within regions of de novo collagen versus ELAC scaffold fibers were counted. Measurements of tissue thickness surrounding the scaffold were also collected.

Collagen Alignment—Slides stained with PSR were placed between a polarizer and analyzed to capture brightfield (polarizer and analyzer in parallel) and dark field images (polarizer and analyzer crossed). After conversion to grayscale, thresholds were determined for brightfield (pixel intensity range, 50–255) and polarized (pixel intensity range, 15–255) images using ImageJ (National Institutes of Health). Black and white pixel counts from threshold images were then used to determine the fraction of aligned collagen within the overall tissue (polarized pixel count/brightfield pixel count = total collagen alignment, “0” = no alignment, and “1” = complete alignment).

Histological Scoring—Stained slides were examined and scored by the senior author and a pathologist (O.A. and J.M.A., respectively) in accordance with modified International Organization for Standardization 10993–6 and American Society for Testing and Materials F981–04 standards.[10,17] Metrics associated with tendon tissue—such as collagen fiber structure and alignment, rounding of nuclei, cell population, and chronic inflammation—were each scored from 0 to 3, based on qualifications from previously published methods,[2,6,41] with a score of 0 in each category representing native tendon. For groups containing scaffolds, regions of the tissue surrounding the exterior structure of the scaffold were similarly scored.

In addition to semiquantitative scoring, cellularity and cell elongation measures were collected from high-power field images of the tissue within the regions of repair from separate slides of each histological specimen (minimum of 12 regions per group).

Immunohistochemistry—Immunohistochemistry was performed for collagen type 1 (dilution, 1:100; collagen 1 alpha 1 antibody; catalog No. NB600–450; Novus Biologicals), collagen type 3 (dilution, 1:100; collagen 3 alpha 1 antibody; catalog No. NBP1–05119; Novus Biologicals), tenomodulin (dilution, 1:50; tenomodulin antibody aa74–123; Horseradish Peroxidase (HRP) conjugated; catalog No. LS-C452705; LifeSpan BioSciences), and matrix metalloproteinase 9 (MMP-9) (dilution, 1:50; catalog No. sc-393859; Santa Cruz Biotechnology). A conjugated secondary antibody (dilution, 1:500; Goat anti-Mouse Immunoglobulin G (IgG) HRP; catalog No. HAF007; Novus Biologicals) was utilized with unconjugated primary antibodies (collagen 1, collagen 3, and MMP-9).

Statistical Analysis

Results collected from biomechanical testing were assessed via Minitab (Version 19.2020.1; Minitab, LLC) using Wilcoxon signed rank tests when comparing operative with intact, contralateral shoulders for animals within a single group. Intergroup comparisons of histological, microCT, and biomechanical data were assessed for significant differences using the Kruskal-Wallis test; where significance was indicated, pairwise comparisons were performed among treatment groups using the Mann-Whitney U test after adjusting for multiple comparisons. For all comparisons, $P < .05$ was used to indicate significant differences between groups, while $P < .1$ indicated marginally significant differences.

RESULTS

ELAC Scaffolds Prevent Tendon Retraction Over Time In Vivo

The analysis of tendon and scaffold retraction (Figure 2A) demonstrated significant tendon retraction in the direct repair group when compared with both ELAC and ELAC + MSC groups, which demonstrated no apparent retraction (combined scaffold groups; $P = .014$). Isolation of the infraspinatus tendon/muscle and the humeri from scapulohumeral complexes after microCT showed no repair failures (Figure 2B).

ELAC Scaffolds Supplemented With MSCs Demonstrate Improved Mechanical Properties for Repaired Infraspinatus Tendons

All constructs in the direct and gap groups failed at the tendon-bone interface. In scaffold groups, 78.6% (n = 11/14) of specimens failed at the bone-scaffold interface, 14.3% (n = 2/14) failed in the midsubstance of the scaffold, and 7.1% (n = 1/14) failed at the musculotendinous junction. Displacement at failure was higher for operative shoulders in all groups (>4 mm) in comparison to contralateral control shoulders (2–3 mm).

Biomechanically, MSC-seeded repairs were found to have comparable maximum load to failure to contralateral control shoulders ($P = .554$). In contrast, specimens in ELAC alone ($P = .052$), direct repair ($P = .036$), and gap groups ($P = .100$) exhibited maximum load to failure values inferior to contralateral control shoulders (Figure 3 and Table 1). Stiffness, modulus, and failure stress measures were significantly lower for all operative shoulders when compared with control shoulders (Table 1). No significant difference in stiffness was appreciated between treatment groups, ranging from 15% to 30% of the stiffness of intact tendons. The modulus of ELAC + MSCs (5.6 ± 2.1 MPa) was similar to that of direct repairs

(5.3 ± 1.3 MPa; P = .713) but significantly higher than that of the ELAC group (3.5 ± 0.4 MPa; $P = .066$). Similarly, failure stress of the ELAC + MSC (9 ± 3.2 MPa) group was similar to that of the direct repair (8 ± 2.5 MPa; $P = .713$) group but significantly higher than that of the ELAC group (3.8 ± 0.9 MPa; $P = .066$).

Tendon Regenerated in and Around ELAC Scaffolds Exhibits Histochemical and Immunohistochemical Properties Similar to Native Tendon

MT staining revealed abundant collagen deposition around the periphery of implanted ELAC scaffolds (Figure 4; outside). On qualitative assessment, collagen deposition was comparatively less abundant within the continuum of the scaffold structure (Figure 4; inside). For direct repair shoulders, collagen was present in the remnant tendon and within the repair site, but it was less distinguishable via MT staining (Figure 4; direct repair).

Point counts (Figure 5) indicated more remodeling in ELAC + MSC specimens, as the volume fraction of collagen threads was significantly lower when compared with the ELAC group (7% vs 37%, respectively; $P = .002$). Stem cell seeding resulted in a nearly 4-fold greater volume fraction of de novo collagen outside the scaffold (ELAC, 16%; ELAC + MSCs, 62% [$P = .003$]). A marginal decrease in de novo collagen within the scaffold region was noted for ELAC + MSC repairs as compared with ELAC repairs (31% vs 47%, respectively; $P = .061$). Measurements of outer layer tissue thickness showed a 130% thicker layer of tissue in the ELAC + MSC specimens when compared with ELAC specimens ($P < .001$).

Quantification of polarized images of PSR-stained sections (Figure 6) compared the degree of collagen alignment and confirmed that collagen alignment in the ELAC 1 MSC (outside) group was similar to that of the native tendon ($P = .166$), while collagen in the ELAC (outside) group was significantly less aligned compared with that in the native tendon ($P = .018$).

Semiquantitative histological scoring demonstrated that the ELAC + MSC group was similar to the 3 other groups, while the direct repair and ELAC groups were significantly more “tendon-like” in appearance as compared with the gap group (Figure 7B). Measurements of cell elongation revealed that the native tendon was distinct from all groups, while cells in the ELAC and ELAC + MSC groups were significantly more elongated than cells in the gap or direct repair groups (Figure 7B; $P < .001$). Cellularity of ELAC + MSC specimens was significantly greater than all groups except for the ELAC group ($P = .063$). Direct repair specimens had the lowest cellularity when compared with all other treatment groups ($P < .05$).

Immunohistochemical staining confirmed type 1 collagen to be present in all groups, with more prominent staining in the ELAC + MSC group compared with the other treatment groups (Figure 7A). Tenomodulin was present in the ELAC and ELAC + MSC groups, with more staining noted in the ELAC + MSC group. Tenomodulin was absent in the direct repair and gap specimens. Collagen type 3 was present in all repair groups, with abundant staining in the gap and direct repair groups and minimal staining in the ELAC and ELAC + MSC groups. Minimal, if any, staining for MMP-9 was noted in the direct repair, ELAC, and

ELAC + MSC groups, while the gap specimens demonstrated a minor presence of MMP-9 in the adipose tissue within the defect site (Appendix Figure A6, available online).

DISCUSSION

The results from this investigation demonstrate the utilization of ELAC scaffolds in the repair of critically sized defects of the RC in a rabbit model. Retraction of the repaired tendon was nearly eliminated in specimens treated with ELAC scaffolds. The structural strength of the ELAC-based repairs supplemented with MSCs were comparable with the strength of intact contralateral tendons. Tissue formed around and within the ELAC scaffolds showed morphological characteristics of native tendon tissue. MSC supplementation of scaffolds resulted in the enhancement of tendon-specific/related markers—such as tenomodulin and type 1 collagen. Together, these findings demonstrate the potential of ELAC biomaterials supplemented with MSCs in the development of future strategies aimed at regenerating and supplementing tendon strength for large or massive RC tears.

Regeneration of bulk tendon tissue continues to pose a challenge in the fields of tissue engineering and orthopaedic surgery. Previous studies examining rabbit RC tendon repair have been limited by a healing period of only 3 months,[18,27,28] whereas this study affirmed healing over an extended period of 6 months. An increase in the stiffness and maximum load of the intact contralateral shoulders was observed in all groups throughout the study as compared with those in our previous 3-month study.[27] One potential cause of the increase in the strength of intact shoulders between the 3-month and 6-month studies could be increased utilization of the contralateral shoulder because the rabbits may have favored the injured shoulder (Appendix Tables A1 and A2, available online). Future studies of this nature should ideally consider ground-reaction force measurements to assess the engagement of limbs between repaired and intact shoulders.

The integrity of scaffold attachment was maintained for 6 months in vivo under load bearing conditions (see Figure 2). Direct repair of shoulders demonstrated significant retraction of the original tendon—a phenomenon noted in other studies.[32,33] The lack of retraction in the ELAC and ELAC + MSC groups reveals an advantage of using scaffolds to bridge the gap between native tendon tissue and bone. The lack of retraction in the scaffold groups was likely because of a reduction of the overall tension on the repair, emphasizing the necessity of using a bridging biomaterial in the treatment of chronically degenerated RC.

MSC supplementation resulted in significant improvements in healing strength when specimens treated with ELAC + MSCs were compared with their intact contralateral counterparts (Figure 3 and Table 1). Apparent modulus and stress demonstrated the difference in the ELAC + MSC group when compared with the ELAC group, showing that MSC supplementation likely improved structural mechanical properties at the tissue/cellular level. Although the failure load of the ELAC + MSC group matched or exceeded that of the intact tendon in some cases, this occurred at a greater tissue cross-sectional area. Therefore, material level properties (failure stress and modulus) were only about 25% of those of native tissue. It is possible that a longer time point would reveal significant biomechanical

differences between nonseeded and MSC-seeded ELAC groups after complete resorption of the ELAC scaffold, as regenerated tissue would be subjected to 100% of the biomechanical load.

In terms of reporting healing biomechanics statistically, we compared the convergence of the operated shoulder to the intact contralateral in a paired sense, as opposed to comparing the median strength values of treatment groups to each other. A paired comparison was preferred because of the large rabbit-to-rabbit variations in the biomechanical properties of intact shoulders. For the sake of completeness of data presentation, group-to-group comparisons of biomechanical variables in a nonpaired context are provided in the Appendix (Appendix Tables A1–A7, available online). Such comparisons did not show statistically significant differences among the healing strengths of direct repair, ELAC, and ELAC + MSCs. In other words, the overall strength of the repairs containing ELAC scaffolds were similar to that of direct repairs. The direct repair group did not involve segmental resection of tendon, whereas such a resection was performed in the ELAC-treated groups. As a result, the direct repair group was at an advantage from the point of view of maintaining the baseline tendon stock, but at the same time, it was also at a disadvantage from the standpoint of being subjected to increased tension to reapproximate the native enthesis. This increased tension may have resulted in more pain and a reduction in utilization of the operative limb for the groups lacking the scaffold. In fact, overutilization of the contralateral shoulder in the direct repair groups could be one reason that the intact controls showed an apparent, but not statistically significant, increase in maximum load to failure (Appendix Table A3, available online).

Histological examinations of the ELAC and ELAC + MSC groups demonstrated robust de novo collagen production (see Figure 4) and the presence of tenomodulin in the neotissue within the continuum of the scaffold and the neotissue immediately outside of the scaffold structure (Figure 7). Immunohistochemical analyses also revealed that collagen type 1 was present in abundance within the scaffold repair group supplemented with MSCs (Figure 7). The gap and direct repair groups exhibited more collagen type 3, while collagen type 3 deposition was minimal in both ELAC scaffold groups (Figure 7A). Coupled with the abundance of tenomodulin within the tissue surrounding the scaffolds, these results suggest that the neotissue within and surrounding the ELAC scaffold structure was the result of tendon-like tissue regeneration as opposed to a progression through fibrous tissue and scar remodeling. Based on results from the present study, topographically tenoinductive effects of ELAC elucidated by previous studies in vitro [20,23,45] persist in vivo over an extended period. Additionally, MMP-9 appeared to be absent in all of the operative groups except for the gap specimens and was indicative of the later stages of healing in the tendon as the initial inflammation was resolved by 6 months after surgery.[29,34,38,39]

The alignment of de novo collagen was also of interest, as there was a significant degree of collagen fiber alignment in the tissue outside the continuum of the scaffolds (Figure 6). The disparity in collagen fiber alignment between the inside and outside of the scaffold is almost entirely a result of the weaving pattern employed to fabricate the scaffold. ELAC scaffolds consisted of weft fibers oriented perpendicular to the plane of histological sections, along with weave fibers oriented parallel to this plane (along the physiological loading axis

of the tendon). Cells attached to ELAC threads elongated and synthesized de novo collagen parallel to the longer axes of the threads. Scaffolds composed of more fibers aligned along the load-bearing axis, as the native tendon would also provide substantial benefits in terms of improving stiffness, which at present was limited to one-third of the native tendon.

Stereological point counting showed that ELAC thread resorption in the ELAC + MSC group was greater than that in the ELAC group, indicating that a greater share of mechanical loading was likely borne by de novo tissue in the ELAC + MSC group. Despite decreased contribution from the scaffold material, MSC-seeded specimens showed increased modulus and failure strength. This result was indicative of restoration of tissue-level biomechanics, as new tissue was subjected to a larger percentage of the mechanical force than were shoulders treated with ELAC alone.

A majority of failures during mechanical testing occurred at the bone-tendon interface, implying that tissue formation in and around the scaffolds was cohesive. However, displacement required to obtain failure was higher in all operative shoulders (>4 mm) when compared with intact contralateral controls (2–3 mm). We hypothesized that limited bone-tendon integration would be a key factor in this finding, as minimal, if any, regeneration of the enthesis was noted during the histological examination. In the context of current approaches to RC repair, special focus should be placed on strategies designed to incorporate spatially arranged elements promoting bone, cartilage, and tendon regeneration to achieve tendon to bone integration comparable with the structure and strength of the native enthesis, as it remains a significant challenge to regenerate in vivo.

This study was not without limitations. While a 6-month period allowed for collagen deposition of the repaired RC defect, histological examination revealed incomplete degradation of the ELAC scaffold, suggesting that further remodeling and regeneration would occur with additional time in vivo. Certain conclusions were based on semiquantitative histological scoring analyses, as is common for in vivo animal models. Point counting was only utilized for comparisons between the scaffold and cell-seeded scaffold groups, whereas point counting of direct repair and healthy control groups was not feasible because these groups inherently did not have an interconnected pore space for cell infiltration—unlike groups with the woven scaffolds. Defects and repairs were acutely induced, limiting the generalizability of our results to degenerative, chronic tears. Future studies of this nature should ideally utilize a chronic failure model involving a 2-step surgical process to induce fatty infiltration by detaching tendon at the enthesis, followed by a second surgery to perform the repair. However, resection of tendon segmentally may defray the limitations of acute injury to some extent by providing a significant regeneration challenge. Sample sizes in treatment groups were uneven, limiting the capability of identifying statistical mechanical differences between direct repair shoulders and their contralateral counterparts. However, the group sizes were selected based on the expected variability in the groups containing the ELAC scaffolds, as the surgical procedure was less straightforward and more subject to variations in healing outcomes, especially in the case of MSC-seeded repairs. Last, there was an apparent lack of biological tendon-bone integration at the native enthesis. The ELAC biotextile was designed to promote tenogenic differentiation; however, this process lacks the ability to promote the integration

of regenerated tendon-like tissue at the native enthesis, which may further improve biomechanical properties.

CONCLUSION

The application of MSCs to ELAC scaffolds has the potential to improve biomechanical and histological outcomes when compared with direct repair for the treatment of critically sized defects of the RC in a rabbit model. ELAC scaffolds could also be utilized in a partial load-bearing context in conjunction with existing repair approaches and materials (ie, FiberTape); and in that context, the contribution of the ELAC scaffold would be in providing biochemical cues to guide organized tissue deposition by infiltrating host cells.

Supplementary Material

Refer to Web version on PubMed Central for supplementary material.

REFERENCES

1. Alfredo Uquillas J, Kishore V, Akkus O. Genipin crosslinking elevates the strength of electrochemically aligned collagen to the level of tendons. J Mech Behav Biomed Mater. 2012;15:176–189. doi:10.1016/j.jmbbm.2012.06.012 [PubMed: 23032437]
2. Aström M, Rausing A. Chronic Achilles tendinopathy: a survey of surgical and histopathologic findings. Clin Orthop Relat Res. 1995;316:151–164. doi:10.1097/00003086-199507000-00021
3. Awad HA, Boivin GP, Dressler MR, Smith FNL, Young RG, Butler DL. Repair of patellar tendon injuries using a cell-collagen composite. J Orthop Res. 2003;21(3):420–431. doi:10.1016/S0736-0266(02)00163-8 [PubMed: 12706014]
4. Awad HA, Butler DL, Harris MT, et al. In vitro characterization of mesenchymal stem cell-seeded collagen scaffolds for tendon repair: effects of initial seeding density on contraction kinetics. J Biomed Mater Res. 2000;51(2):233–240. doi:10.1002/(SICI)1097-4636(200008)51:2\233:AID-JBM12.3.0.CO;2-B [PubMed: 10825223]
5. Chaudhury S, Dines JS, Delos D, Warren RF, Voigt C, Rodeo SA. Role of fatty infiltration in the pathophysiology and outcomes of rotator cuff tears. Arthritis Care Res. 2012;64(1):76–82. doi:10.1002/acr.20552
6. Chen JM, Willers C, Xu J, Wang A, Zheng M-H. Autologous tenocyte therapy using porcine-derived bioscaffolds for massive rotator cuff defect in rabbits. Tissue Eng. 2007;13(7):1479–1491. doi:10.1089/ten.2006.0266 [PubMed: 17536925]
7. Cheng X, Gurkan UA, Dehen CJ, et al. An electrochemical fabrication process for the assembly of anisotropically oriented collagen bundles. Biomaterials. 2008;29(22):3278–3288. doi:10.1016/j.biomaterials.2008.04.028 [PubMed: 18472155]
8. Colvin AC, Egorova N, Harrison AK, Moskowitz A, Flatow EL. National trends in rotator cuff repair. J Bone Joint Surg Am. 2012;94(3):227–233. doi:10.2106/JBJS.J.00739 [PubMed: 22298054]
9. Ek ETH, Neukom L, Catanzaro S, Gerber C. Reverse total shoulder arthroplasty for massive irreparable rotator cuff tears in patients younger than 65 years old: results after five to fifteen years. J Shoulder Elbow Surg. 2013;22(9):1199–1208. doi:10.1016/j.jse.2012.11.016 [PubMed: 23385083]
10. F04 Committee. Practice for assessment of compatibility of biomaterials for surgical implants with respect to effect of materials on muscle and bone. ASTM International. Accessed August 26, 2020. doi:10.1520/F0981-04R16
11. Fessel G, Gerber C, Snedeker JG. Potential of collagen cross-linking therapies to mediate tendon mechanical properties. J Shoulder Elbow Surg. 2012;21(2):209–217. doi:10.1016/j.jse.2011.10.002 [PubMed: 22244064]

12. Galatz LM, Ball CM, Teefey SA, Middleton WD, Yamaguchi K. The outcome and repair integrity of completely arthroscopically repaired large and massive rotator cuff tears. J Bone Joint Surg Am. 2004;86(2):219–224. doi:10.2106/00004623-200402000-00002 [PubMed: 14960664]
13. Gillespie RJ, Knapik DM, Akkus O. Biologic and synthetic grafts in the reconstruction of large to massive rotator cuff tears. J Am Acad Orthop Surg. 2016;24(12):823–828. doi:10.5435/JAAOS-D-15-00229 [PubMed: 27768610]
14. Gladstone JN, Bishop JY, Lo IKY, Flatow EL. Fatty infiltration and atrophy of the rotator cuff do not improve after rotator cuff repair and correlate with poor functional outcome. Am J Sports Med. 2007;35(5):719–728. doi:10.1177/0363546506297539 [PubMed: 17337727]
15. Gomoll AH, Katz JN, Warner JJP, Millett PJ. Rotator cuff disorders: recognition and management among patients with shoulder pain. Arthritis Rheum. 2004;50(12):3751–3761. doi:10.1002/art.20668 [PubMed: 15593187]
16. Han B, Jones IA, Yang Z, Fang W, Vangsness CT. Repair of rotator cuff tendon defects in aged rats using a growth factor injectable gel scaffold. Arthroscopy. 2020;36(3):629–637. doi:10.1016/j.arthro.2019.09.015 [PubMed: 31784364]
17. International Organization for Standardization. Biological evaluation of medical devices—Part 6: Tests for local effects after implantation. ISO 10993–6:2016. Accessed August 26, 2020. https://www.iso.org/cms/render/live/en/sites/isoorg/contents/data/standard/06/10/61089.html
18. Inui A, Kokubu T, Fujioka H, et al. Application of layered poly (L-lactic acid) cell free scaffold in a rabbit rotator cuff defect model. Sports Med Arthrosc Rehabil Ther Technol. 2011;3(1):29. doi:10.1186/1758-2555-3-29 [PubMed: 22136125]
19. Islam A, Bohl MS, Tsai AG, Younesi M, Gillespie R, Akkus O. Biomechanical evaluation of a novel suturing scheme for grafting load-bearing collagen scaffolds for rotator cuff repair. Clin Biomech. 2015;30(7):669–675. doi:10.1016/j.clinbiomech.2015.05.007
20. Islam A, Younesi M, Mbimba T, Akkus O. Collagen substrate stiffness anisotropy affects cellular elongation, nuclear shape, and stem cell fate toward anisotropic tissue lineage. Adv Healthc Mater. 2016;5(17):2237–2247. doi:10.1002/adhm.201600284 [PubMed: 27377355]
21. Juncosa-Melvin N, Boivin GP, Gooch C, et al. The effect of autologous mesenchymal stem cells on the biomechanics and histology of gel-collagen sponge constructs used for rabbit patellar tendon repair. Tissue Eng. 2006;12(2):369–379. doi:10.1089/ten.2006.12.369 [PubMed: 16548695]
22. Kikinis R, Pieper SD, Vosburgh KG. 3D Slicer: a platform for subject-specific image analysis, visualization, and clinical support. In: Jolesz FA, ed. Intraoperative Imaging and Image-Guided Therapy. Springer; 2014:277–289. doi:10.1007/978-1-4614-7657-3_19
23. Kishore V, Bullock W, Sun X, Van Dyke WS, Akkus O. Tenogenic differentiation of human MSCs induced by the topography of electrochemically aligned collagen threads. Biomaterials. 2012;33(7):2137–2144. doi:10.1016/j.biomaterials.2011.11.066 [PubMed: 22177622]
24. Kishore V, Uquillas JA, Dubikovsky A, et al. In vivo response to electrochemically aligned collagen bioscaffolds. J Biomed Mater Res B Appl Biomater. 2012;100(2):400–408. doi:10.1002/jbm.b.31962 [PubMed: 22179969]
25. Klatte-Schulz F, Gerhardt C, Scheibel M, Wildemann B, Pauly S. Relationship between muscle fatty infiltration and the biological characteristics and stimulation potential of tenocytes from rotator cuff tears. J Orthop Res. 2014;32(1):129–137. doi:10.1002/jor.22481 [PubMed: 24022826]
26. Lamberti PM, Wezeman FH. Biologic behavior of an in vitro hydrated collagen gel–human tenocyte tendon model. Clin Orthop Relat Res. 2002;397:414–423. doi:10.1097/00003086-200204000-00049
27. Learn GD, McClellan PE, Knapik DM, et al. Woven collagen biotextiles enable mechanically functional rotator cuff tendon regeneration during repair of segmental tendon defects in vivo. J Biomed Mater Res B Appl Biomater. 2019;107(6):1864–1876. doi:10.1002/jbm.b.34279 [PubMed: 30485649]
28. Liu G-M, Pan J, Zhang Y, et al. Bridging repair of large rotator cuff tears using a multilayer decellularized tendon slices graft in a rabbit model. Arthroscopy. 2018;34(9):2569–2578. doi:10.1016/j.arthro.2018.04.019 [PubMed: 30078689]

29. Loiselle AE, Frisch BJ, Wolenski M, et al. Bone marrow-derived matrix metalloproteinase-9 is associated with fibrous adhesion formation after murine flexor tendon injury. PLoS ONE. 2012;7(7): e40602. doi:10.1371/journal.pone.0040602 [PubMed: 22792383]
30. Mandarim-de-Lacerda CA. Stereological tools in biomedical research. An Acad Bras Ciênc. 2003;75(4):469–486. doi:10.1590/S0001-37652003000400006 [PubMed: 14605681]
31. Marcos R, Monteiro RA, Rocha E. The use of design-based stereology to evaluate volumes and numbers in the liver: a review with practical guidelines. J Anat. 2012;220(4):303–317. doi:10.1111/j.1469-7580.2012.01475.x [PubMed: 22296163]
32. Mazzocca AD, Bollier MJ, Obopilwe E, et al. Biomechanical evaluation of arthroscopic rotator cuff repairs over time. Arthroscopy. 2010;26(5):592–599. doi:10.1016/j.arthro.2010.02.009 [PubMed: 20434655]
33. Meyer DC, Lajtai G, von Rechenberg B, Pfirrmann CWA, Gerber C. Tendon retracts more than muscle in experimental chronic tears of the rotator cuff. J Bone Joint Surg Br. 2006;88(11):1533–1538. doi:10.1302/0301-620X.88B11.17791 [PubMed: 17075105]
34. Minkwitz S, Schmock A, Kurtoglu A, et al. Time-dependent alterations of MMPs, TIMPs and tendon structure in human Achilles tendons after acute rupture. Int J Mol Sci. 2017;18:2199–2212. doi:10.3390/ijms18102199 [PubMed: 29053586]
35. Mitchell C, Adebajo A, Hay E, Carr A. Shoulder pain: diagnosis and management in primary care. BMJ. 2005;331(7525):1124–1128. doi:10.1136/bmj.331.7525.1124 [PubMed: 16282408]
36. Piper CC, Hughes AJ, Ma Y, Wang H, Neviaser AS. Operative versus nonoperative treatment for the management of full-thickness rotator cuff tears: a systematic review and meta-analysis. J Shoulder Elbow Surg. 2018;27(3):572–576. doi:10.1016/j.jse.2017.09.032 [PubMed: 29169957]
37. Rees JL. The pathogenesis and surgical treatment of tears of the rotator cuff. J Bone Joint Surg Br. 2008;90(7):827–832. doi:10.1302/0301-620X.90B7.19874 [PubMed: 18591587]
38. Robertson CM, Chen CT, Shindle MK, Cordasco FA, Rodeo SA, Warren RF. Failed healing of rotator cuff repair correlates with altered collagenase and gelatinase in supraspinatus and subscapularis tendons. Am J Sports Med. 2012;40(9):1993–2001. doi:10.1177/0363546512456519 [PubMed: 22896627]
39. Rodeo SA. Biologic augmentation of rotator cuff tendon repair. J Shoulder Elbow Surg. 2007;16(suppl 5):S191–S197. doi:10.1016/j.jse.2007.03.012 [PubMed: 17574875]
40. Schipke J, Brandenberger C, Rajces A, et al. Assessment of cardiac fibrosis: a morphometric method comparison for collagen quantification. J Appl Physiol. 2017;122(4):1019–1030. doi:10.1152/japplphysiol.00987.2016 [PubMed: 28126909]
41. Shen W, Chen J, Yin Z, et al. Allogenous tendon stem/progenitor cells in silk scaffold for functional shoulder repair. Cell Transplant. 2012;21(5):943–958. doi:10.3727/096368911X627453 [PubMed: 22405331]
42. Uquillas JA, Akkus O. Modeling the electromobility of type-I collagen molecules in the electrochemical fabrication of dense and aligned tissue constructs. Ann Biomed Eng. 2012;40(8):1641–1653. doi:10.1007/s10439-012-0528-1 [PubMed: 22314838]
43. Valencia AP, Lai JK, Iyer SR, et al. Fatty infiltration is a prognostic marker of muscle function after rotator cuff tear. Am J Sports Med. 2018;46(9):2161–2169. doi:10.1177/0363546518769267 [PubMed: 29750541]
44. Yang G, Rothrauff BB, Tuan RS. Tendon and ligament regeneration and repair: clinical relevance and developmental paradigm. Birth Defects Res Part C Embryo Today Rev. 2013;99(3):203–222. doi:10.1002/bdrc.21041
45. Younesi M, Islam A, Kishore V, Anderson JM, Akkus O. Tenogenic induction of human MSCs by anisotropically aligned collagen biotextiles. Adv Funct Mater. 2014;24(36):5762–5770. doi:10.1002/adfm.201400828 [PubMed: 25750610]

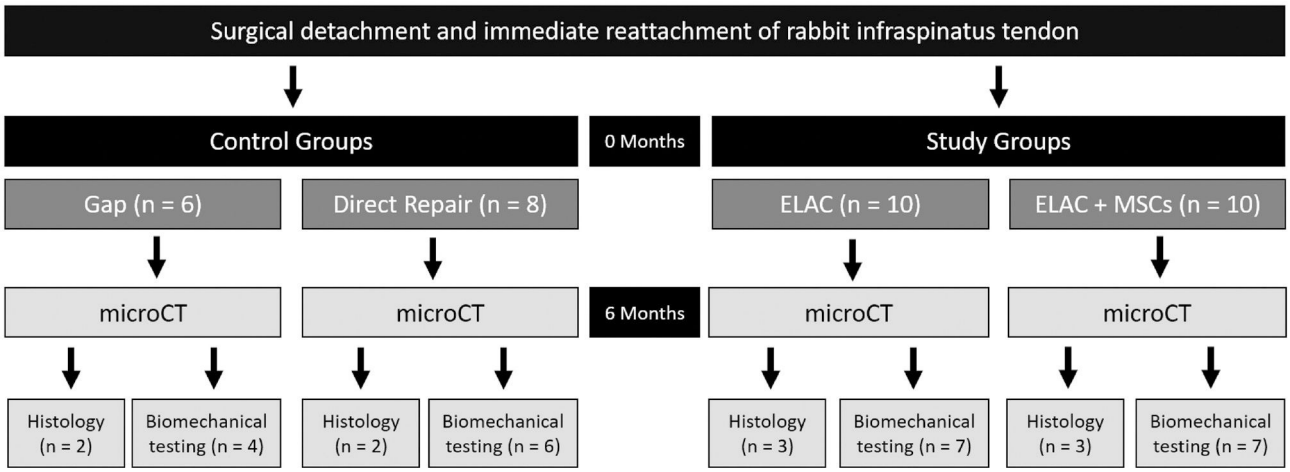

Figure 1.

Study design, groups, and analyses. ELAC, electrochemically aligned collagen; microCT, micro–computed tomography; MSC, mesenchymal stem cell.

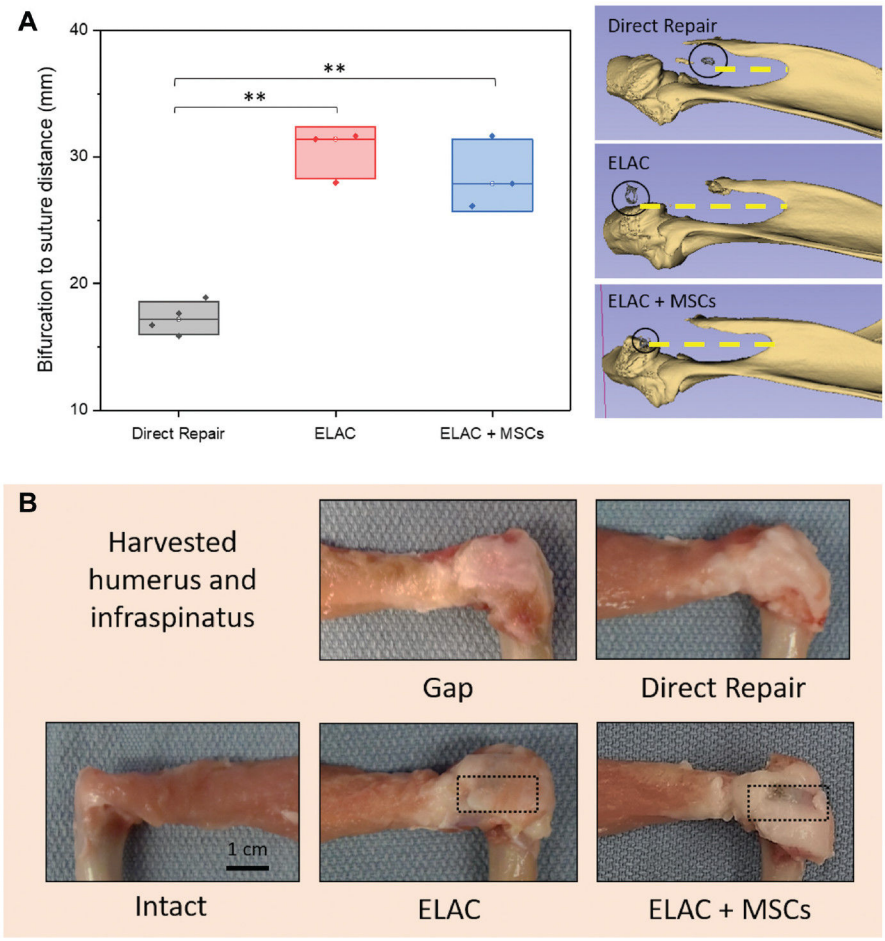

Figure 2.

(A) The distance between the scapular bifurcation and the stainless steel suture marker (circled) at the distal end of the repaired tendon is highlighted by a yellow dashed line. This distance is inversely proportional to tendon retraction that was measured using micro–computed tomography. Significance noted as (**) for $P < .05$. (B) Gross appearance of the isolated humerus and the infraspinatus tendon/muscle. ELAC, electrochemically aligned collagen; MSC, mesenchymal stem cell.

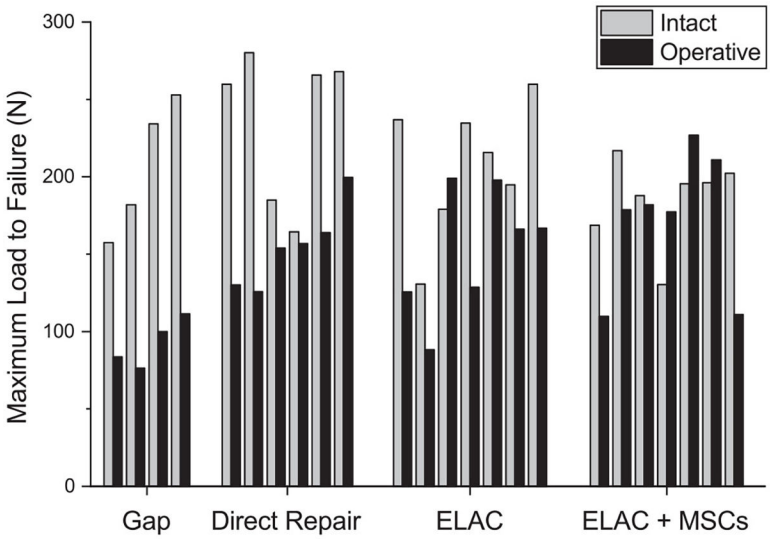

Figure 3.

Maximum load to failure for individual shoulders in each group. Operative specimens were compared with intact, contralateral counterparts. The ELAC + MSC group was the only one that demonstrated no significant differences between operative and intact shoulders with respect to failure load. ELAC, electrochemically aligned collagen; MSC, mesenchymal stem cell.

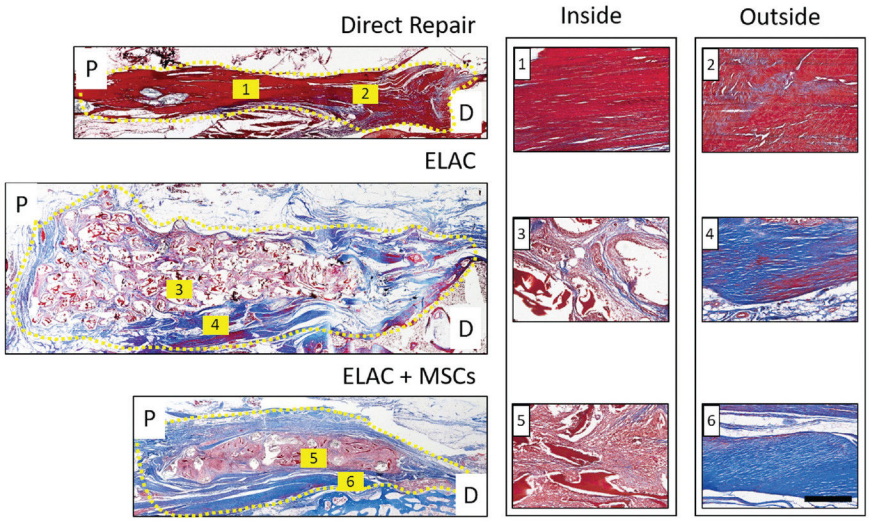

Figure 4.

Representative histological sections of the direct repair, ELAC, and ELAC + MSC groups stained with Masson trichrome (blue depicts de novo and loosely packed collagen; red highlights ELAC and other extracellular matrix components). Proximal (*P*) and distal (*D*) regions are noted, and the region of the repair is highlighted by a dotted yellow line. Collagen was more difficult to distinguish in the direct repair specimens, but it was still visible (blue and red regions overlap in 1 and 2). Collagen within the continuum of the scaffolds for both scaffold groups (faint blue visible in 3 and 5) was not as robust or apparent as collagen in the tissue surrounding the scaffold structure (deep blue present in 4 and 6). Scale bar = 200 mm. ELAC, electrochemically aligned collagen; MSC, mesenchymal stem cell.

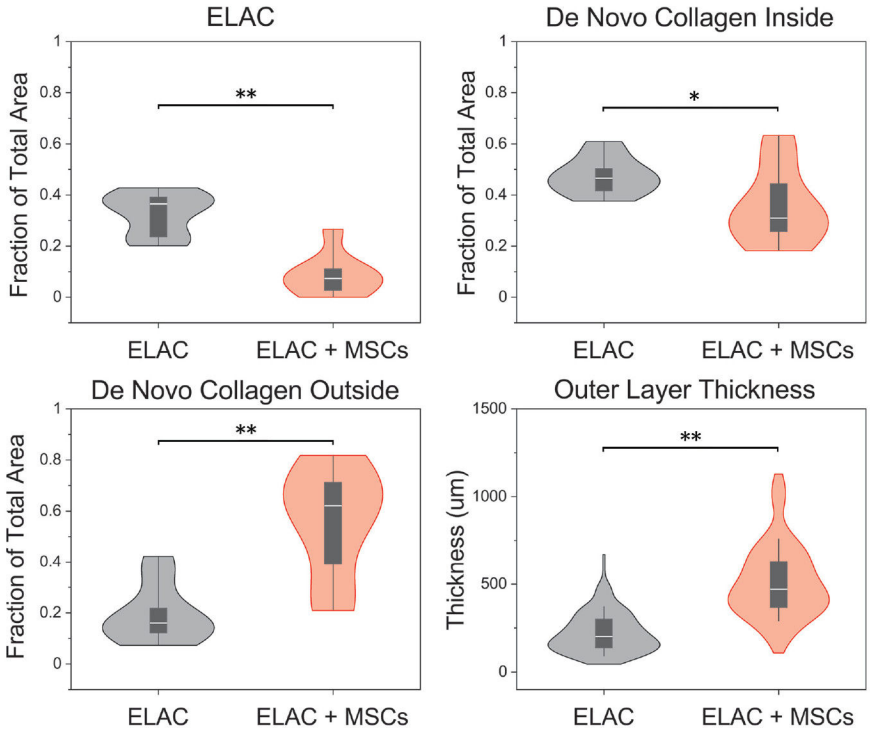

Figure 5.

Violin plots illustrating the distributions of the fraction of total area occupied by ELAC, de novo collagen inside, and de novo collagen outside, as well as measurements of the thickness of the outer layer of tissue surrounding the scaffold. Significantly more de novo collagen outside the continuum of the scaffold structure was noted for the ELAC + MSC group and less of the total area was occupied by ELAC fibers in the ELAC + MSC group. Measurements of the thickness of the layer of tissue surrounding the scaffolds were significantly higher in the ELAC + MSC group. Significance noted as (**) for $P < .05$ and (*) for $.05 \leq P \leq .10$. ELAC, electrochemically aligned collagen; MSC, mesenchymal stem cells.

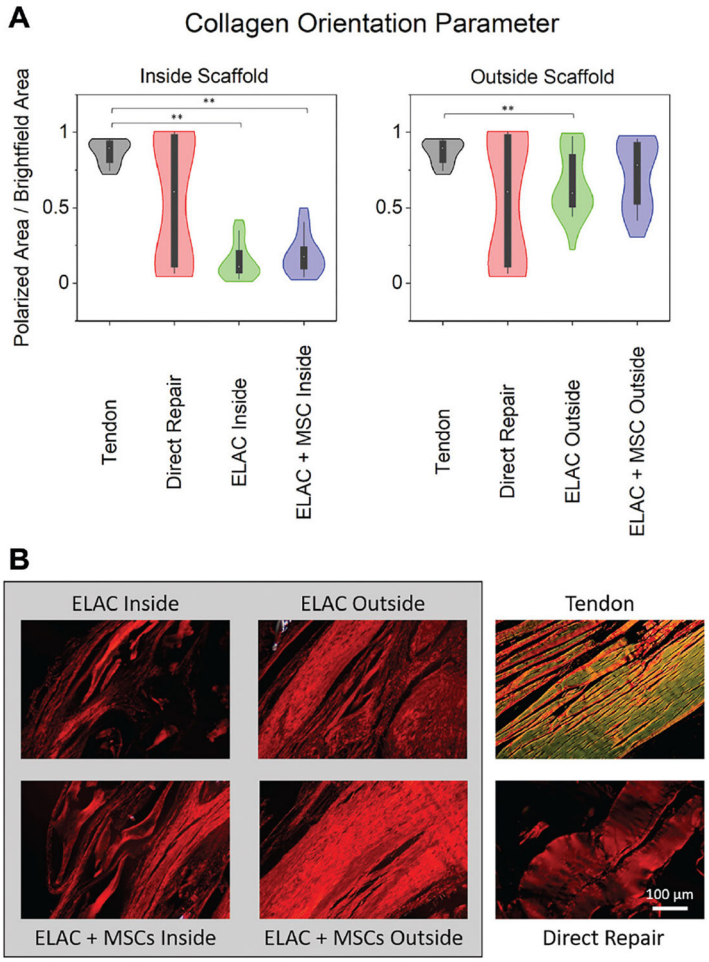

Figure 6.

(A) Violin plots highlighting the distributions for assessment of orientation of the collagen fibers in histological specimens stained with picrosirius red and imaged under polarized and brightfield conditions. On the *y*-axes, “0” indicates no tissue visible under polarized light, and “1” indicates that all of the tissue visible under brightfield conditions is visible under polarized light (or aligned). Collagen within the continuum of the scaffold structure showed significantly lower alignment compared with the native tendon for both scaffold groups; however, collagen outside the continuum of the scaffolds was similar to the native tendon for the ELAC + MSC group. (B) Representative polarized light microscopy images from representative specimens demonstrating the orientation of the collagen fibers. Scale bar = 100 µm. Significance noted as (**) for $P < .05$. ELAC, electrochemically aligned collagen; MSC, mesenchymal stem cell.

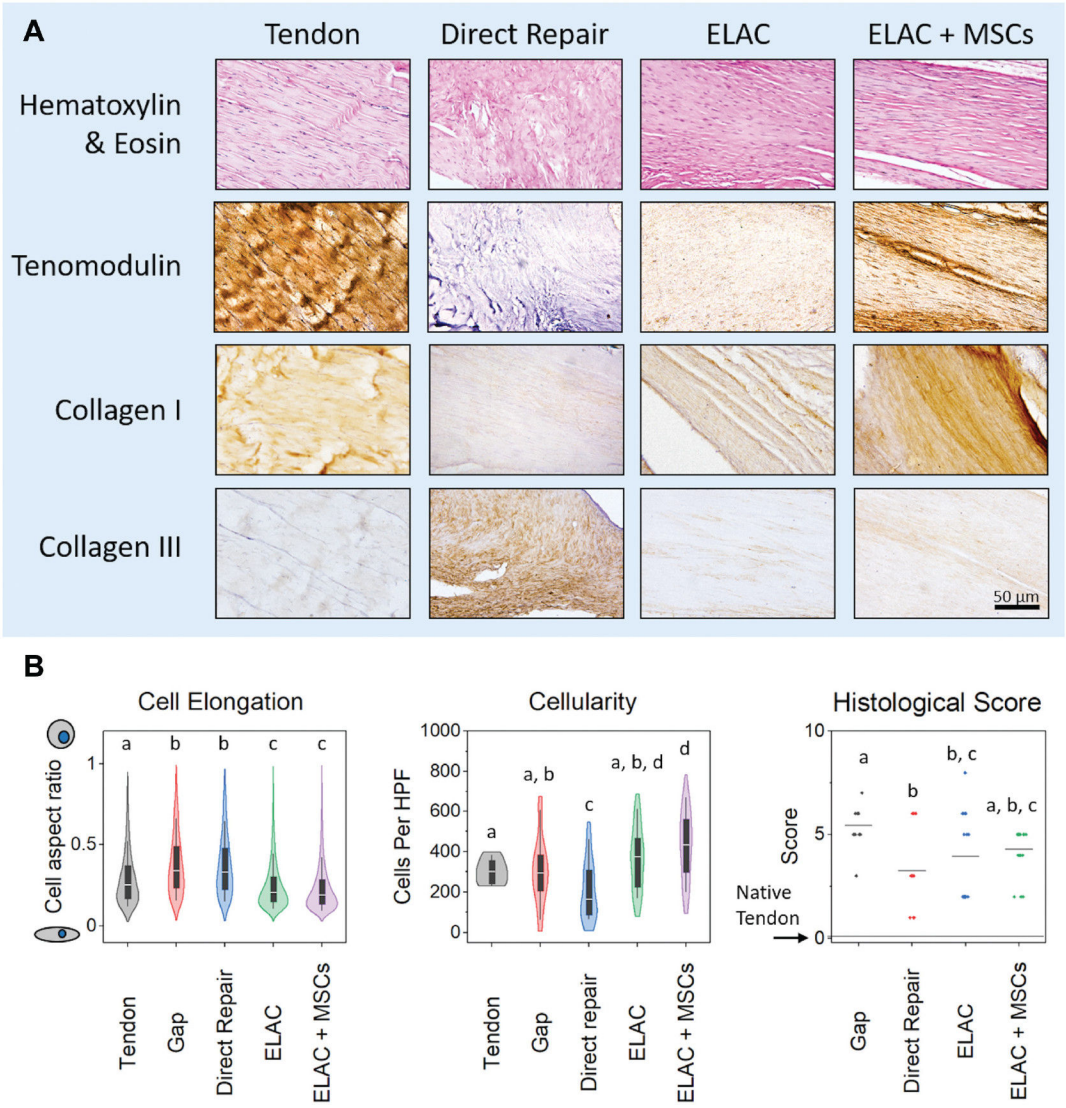

Figure 7.

(A) Histological and immunohistochemical staining. Hematoxylin and eosin staining shows the cellularity and cellular elongation/shape within the tissue surrounding the ELAC scaffolds. Tenomodulin was present in the ELAC and ELAC + MSC groups and notably absent in the direct repair group. Collagen type 1 appeared to be present in greater amounts in the scaffold-containing groups as compared with the direct repair group, and staining for collagen type 3 illustrated the opposite trend (more was present in the direct repair group than in ELAC scaffold groups). Scale bar = 50 µm. (B) Histological metrics. Significantly more cells were elongated in the ELAC and ELAC + MSC groups when compared with the native tendon, gap, and direct repair groups. In terms of cellularity, the direct repair group had the fewest cells per high-power field of view, and the ELAC + MSC group had significantly more cells than all groups except for the ELAC group. Histological scores for tendon-like metrics revealed that the gap group was significantly less tendon-like than the other 3 operative groups (a score of "0" indicates no apparent difference from the native tendon). Significance in (B) is noted by letters above each group in the plot that corresponds

to the grouping. For example, a group denoted with the letter *a* is not statistically different from another group that is also denoted with a. ELAC, electrochemically aligned collagen; MSC, mesenchymal stem cell.

TABLE 1

Statistical Comparisons of Mechanical Properties[a]

Group	Maximum Load, N (median ± SD) (p-value)	Stiffness, N/mm (median ± SD) (p-value)	Modulus, MPa (median ± SD) (p-value)	Failure Stress, MPa
Intact	199 ± 35	144 ± 20	25 ± 3.7	104 ± 7
Gap	92 ± 15 (.100)	21 ± 10 (.100)	NA	NA
Direct	155 ± 22 (.036)	38 ± 12 (.036)	5.3 ± 1.3 (.100)	8 ± 2.5 (.100)
ELAC	166 ± 36 (.052)	33 ± 6 (.022)	3.5 ± 0.4 (.100)	3.8 ± 0.9 (.100)
ELAC + MSC	**178 ± 50 (.554)**	46 ± 12 (.022)	5.6 ± 2.1 (.059)	9 ± 3.2 (.059)

[a]Paired comparisons of biomechanical properties of repaired tendons to those of intact contralateral tendons. Data are reported as median ± SD with p-values in parentheses. The lack of significance in bold implies complete convergence of repair to intact. ELAC, electrochemically aligned collagen; MSC, mesenchymal stem cell; NA, not available.